

**Temporal and spatial variations of surface pCO₂, phosphate, nitrate, and
silicate in the western equatorial Pacific**

Amelia Carothers

University of Washington

School of Oceanography, Box 357940

Seattle WA 98195-7940

acarot@uw.edu

3/8/2024

Abstract:

Nutrients and CO₂ are important oceanographic variables, as they provide information which can be used to understand phytoplankton abundance and processes such as the oceanic carbon cycle. Therefore, as climate change impacts ocean systems, it is increasingly important to measure how nutrient and CO₂ concentrations in the ocean change over time and space. This study measured pCO₂ (which takes into account temperature, total CO₂, salinity, and alkalinity of the water), nitrate, phosphate and silicate concentrations in the western equatorial Pacific (5S-5N along 167W) in January 2024. Over space, pCO₂ and nutrients were analyzed for correlation with physical processes, primarily upwelling, using sea surface temperature (SST) and mixed layer depth. To determine the relationship of pCO₂ and nutrient concentrations to the biomass of microorganisms, correlations with fluorescence and beam transmission were also analyzed over space. Over time, pCO₂ was compared to atmospheric CO₂ and El Niño Southern Oscillation (ENSO) state to determine correlations between temporal pCO₂ trends and atmospheric phenomena. pCO₂ surface concentrations in the western equatorial Pacific were found to have increased from 1983 to 2024 at an average rate of 2.02 ± 0.034 ppm/yr and had a positive correlation with increasing average atmospheric CO₂ (R = 0.71, p-value < 0.001). Spatially, surface pCO₂ and the macronutrients nitrate, phosphate, and silicate in the upper 200 m showed similar patterns from 5S to 5N along 167W. The concentrations of nitrate and phosphate had a significant negative correlation to mixed layer depth (R = -0.4, p-value < 0.001) and nutrients and pCO₂ had a significant negative correlation to sea surface temperature (p-value < 0.001). They peaked from 0-2N due to upwelling and exhibited smaller secondary peaks around 3S and 3N, likely due to mixing caused by north and south subsurface countercurrents. These results

reinforce the importance of physical oceanic and atmospheric processes as a control for nutrient and inorganic carbon cycles in the western equatorial Pacific.

Plain Language Summary:

Carbon dioxide and nutrients affect many biological and chemical processes in the ocean such as primary production and ocean-atmosphere gas exchange. Since climate change is impacting the ocean in multiple ways, it is important to see what affects how CO₂ and nutrient concentrations change over time and space. This study measured CO₂ and nutrient concentrations in the western equatorial Pacific and compared them to physical and biological variables to determine any correlations. The CO₂ concentration in the surface of the western equatorial Pacific was found to increase over time, and that this trend was similar to the increase in CO₂ in the atmosphere. Both nutrients and CO₂ were highest at the equator, with smaller peaks in concentration to the north and south. This pattern is likely due to the movement of deep water to the surface at the equator, and currents mixing deep water with surface water at the locations to the north and south. These results reinforce the idea that physical processes like currents and interactions with the atmosphere have large effects on CO₂ and nutrient concentrations in the equatorial Pacific.

Introduction:

CO₂ is an important component of biogeochemical cycles in the ocean. Besides being taken up by photosynthetic organisms and generated during cellular respiration, CO₂ is also exchanged between the surface ocean and atmosphere and impacts pH (Feely et al., 1999; Pittman et al., 2022; Paytan & Hönisch, 2016). Nutrients are another important part of marine ecosystems and biogeochemical cycles. They are taken up by phytoplankton at the surface and then regenerated in deeper water by microbial processes (Tilman et al., 1982). Due to their importance for growth and maintenance, nitrate, phosphate, and silicate concentrations can act as controlling factors for phytoplankton growth (Tilman et al., 1982). Phytoplankton blooms at the equator can be limited by nitrate and silicic acid concentrations and can reduce dissolved CO₂ concentrations near the surface (Ishii et al., 2009; Talling, 1976). The equatorial Pacific in particular is important for biogeochemical cycling due to the upwelling of deep nutrient and CO₂ rich water to the surface along the equator (Feely et al., 1999; Ishii et al., 2009).

Nutrient and pCO₂ concentrations can have large impacts on ecosystems. For instance, reduced mixing caused by El Niño can limit phytoplankton concentrations by decreasing supply of nutrients from deep water (Gierach et al., 2012; Strutton & Chávez, 2000). Furthermore, increased pCO₂ concentrations could also impact the community structure of phytoplankton, as well as their ability to uptake and utilize nutrients such as nitrate (Tortell et al., 2002). Compromised nutrient uptake would then affect the species present on higher levels of the trophic system by decreasing primary production (Steele & Frost, 1977).

Therefore, it is vital to increase knowledge on CO₂ and nutrient concentration variability in the equatorial Pacific so that future changes, which may impact productivity and carbon cycling, can be predicted. Nutrients and pCO₂ in the equatorial Pacific exhibit natural

intra-annual seasonal variability. Average nitrate and silicate concentrations exhibit a weak peak during March and September (Strutton et al., 2008). Phosphate is more variable, but similarly peaks weakly during the late winter and fall (Strutton et al., 2008). This seasonal change in nutrients is likely due to changes in physical processes including wind driven mixing (Archer et al., 1996).

Multiple oceanic-atmospheric processes such as the El Niño Southern Oscillation (ENSO), Pacific Decadal Oscillation (PDO) and intra-annual wind variability can have an impact on nutrient and dissolved CO₂ concentrations in the equatorial Pacific. These events influence upwelling, surface currents and water masses in the region, which impact the amount of nutrients and dissolved CO₂ in surface waters (Jin, 1997). El Niño is initiated by anomalously high sea surface temperatures (SSTs). These temperatures impact atmospheric circulation by reducing the east-west SST gradient. This causes the easterly trade winds to slow or reverse, which further reduces the SST gradient in a positive feedback loop (Bjerknes, 1969). The slowing and/or reversal of the trade winds means that less water flows away from the equator due to Ekman transport driven by these winds. Therefore, less deep water upwells to the surface at the equator which decreases the extent of cold, nutrient and CO₂ rich upwelled water in the western equatorial Pacific (Bjerknes, 1969).

Temporal variations in dissolved CO₂ and nutrients in the equatorial Pacific are often driven by ENSO. During an El Niño period, less divergence of surface water occurs, leading to a lower amount of upwelling, and slowing of the equatorial undercurrent (EUC) (Kessler & McPhaden, 1995). pCO₂ (partial pressure of carbon dioxide, which unlike dissolved CO₂ is also influenced by temperature, total CO₂, salinity, and alkalinity) and nutrients at the equator decline during El Niño due to this decreased upwelling (Yasunaka et al., 2019; Wong et al., 1993;

Strutton et al., 2008). In fact, ENSO is the driving force behind dissolved CO₂ changes inter-annually (Sutton et al., 2014). For instance, outgassing of CO₂ at the equator varies by ~50% between El Niño and non El Niño years. These ENSO-driven changes impact the chemical oceanography of the region, as less nutrients and pCO₂ are delivered by upwelling and mixed into surface waters (Stramma et al., 2016; Wong et al., 1993; Barber et al., 1994).

The PDO is another climate phenomena which can impact the water masses of the western equatorial Pacific. It is driven by a combination of forces such as ocean heat flux, Ekman transport driven by the Aleutian low, and changes in the Kuroshio-Oyashio current system, however it is still not completely understood (Newman et al., 2016). The PDO represents the prominent long-term pattern of North Pacific SST variability. It has a negative and positive phase which correspond to warm and cool SST anomalies respectively and tend to last 20-30 years (Newman et al., 2016). It is possible the PDO may impact surface current strength and upwelling over decadal time scales due to changes in SST gradient (Yasunaka et al., 2019). Such variations in the physical characteristics of the equatorial region caused by phenomena like ENSO, and possibly the PDO, can impact nutrient concentrations and dissolved CO₂ (Yasunaka et al., 2019).

There is also a long-term trend from 1981 to 2015 of increasing pCO₂ at the equator, possibly related to PDO forcing (Yasunaka et al., 2019; Wong et al., 1993). Across the equator, measured pCO₂ concentrations increased 2.3 to 3.3 μatm/yr and pH decreased 0.0018 to 0.0026 yr⁻¹ across the region from 1997 to 2011 (Sutton et al., 2014). In the western equatorial Pacific specifically, pCO₂ increased on average 1.5±0.2 μatm/year between 1985 and 2004 (Ishii et al., 2009). There is disagreement as to whether this increase is actually caused by PDO forcing, as increasing surface pCO₂ often mirrors atmospheric CO₂ increase (Sutton et al., 2014).

Anthropogenic climate change is another factor which is influencing the chemical and physical properties of the Pacific over time. As more CO₂ is being released into the atmosphere by the combustion of fossil fuels, pCO₂ is increasing in many parts of the ocean as the ocean acts as a sink for CO₂ (Sutton et al., 2014). This lowers pH, which can harm many organisms, especially those which form calcium carbonate shells (Meyer & Riebesell, 2015). In addition, increasing atmospheric temperatures caused by greenhouse gasses are impacting weather patterns and ocean SST, which may in turn impact physical properties such as upwelling events due to changes in wind and surface currents (Kang et al., 2023). However, due to the complexities of increasing SST, Antarctic meltwater discharge, and other variables, the extent of the impact of future SST gradient changes is yet unknown (Kang et al., 2023).

Both pCO₂ and nutrients also vary spatially across the equator. The cold tongue, located east of 140W and from 3N - 15S, tends to have higher nutrients, pCO₂ and lower temperatures due to the upwelling deep water. From 2000 to 2020, CO₂ flux into the atmosphere increased in the cold tongue region but decreased everywhere else (Pittman et al., 2022). Nitrate, phosphate, and silicate concentrations decrease from east to west across the equatorial Pacific (Strutton et al., 2008; Pittman et al., 2022). The concentrations of these nutrients, along with other properties such as temperature, salinity, density, and biological abundance vary across the three main water masses at the equator (Pittman et al., 2022). In contrast to the cold tongue along the eastern equator, the warm pool in the east (3N-15N) and the warm pool to the west of 140W have higher temperatures and generally lower pCO₂ and nutrient concentrations due to a lower amount of mixing between deep and surface layers because of the steeper thermocline (Pittman et al., 2022). The high-nutrient cold tongue can extend to ~180E and enables primary producers to survive at higher concentrations in the area (Murray et al., 1992).

With climate change affecting both physical and chemical dynamics in the world's oceans, it is vital to update existing data on how chemical properties are changing over time in the equatorial region. By understanding long term trends and variability of $p\text{CO}_2$ and nutrients, we can better predict how exactly this region will affect and be affected by increasing atmospheric CO_2 levels due to anthropogenic factors. Therefore, the goal of this study is to add to previously collected data to better understand drivers of spatial and temporal variations in nutrients and surface $p\text{CO}_2$ in the western equatorial Pacific. This will be done by identifying possible correlations with the physical processes of upwelling and mixing, and microorganism biomass. Beam transmission and fluorescence were chosen as proxies for total microorganism biomass and photosynthetic microorganism biomass respectively. Nitrate, phosphate and silicate were chosen because these nutrients can sometimes control the growth of phytoplankton communities in the equatorial region (Ishii et al., 2009; Tilman et al., 1982).

I hypothesize measured nutrient concentrations and $p\text{CO}_2$ will be highest on the equator due to upwelling. $p\text{CO}_2$ will follow the trend of an average increase when compared to previous years. Both nutrients and $p\text{CO}_2$ will have higher correlation with physical variables related to upwelling such as temperature and mixed layer depth and have lower correlation with biological indicators.

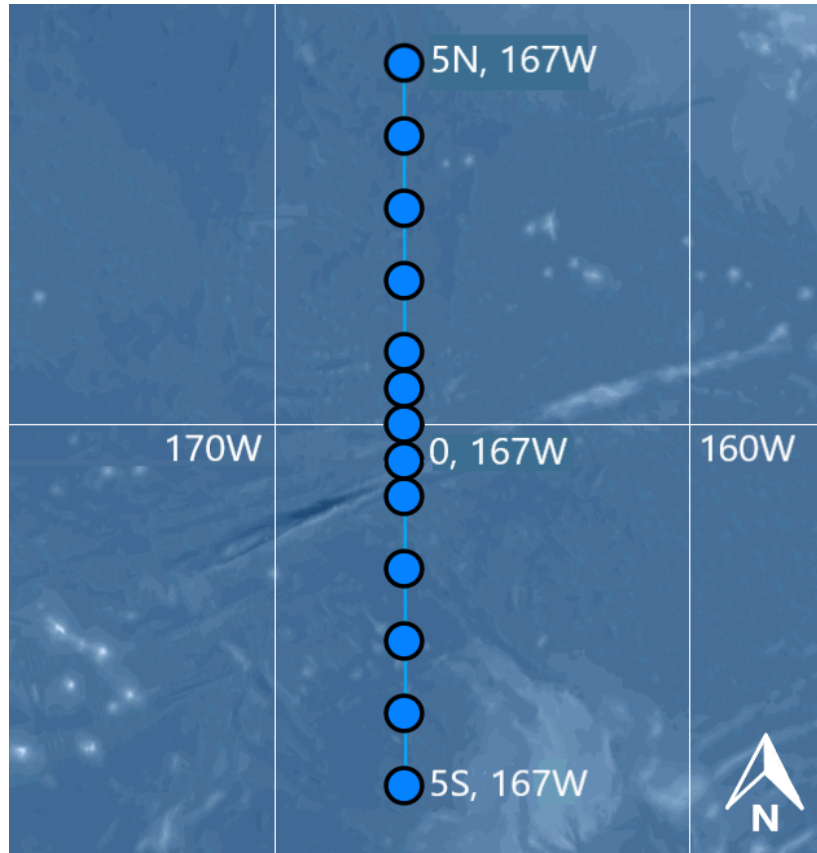


Figure 1. Map depicting the transect and stations sampled on cruise TN427, January 2024.

Methods:

Cruise Data

Data was collected during the University of Washington oceanography senior thesis cruise TN427 from Dec. 29th 2023 to Jan. 10th 2024 out of Pago Pago American Samoa.

Nutrients

Nutrients were collected from each of the 13 stations (5S, 4S, 3S, 2S, 1S, 0.5S, 0, 0.5N, 1N, 2N, 3N, 4N, 5N) along the transect from 5S to 5N (Fig. 1). Nine nutrient samples were collected from each of the stations, the depths of which were chosen based on the depth of the mixed layer and the depth of the equatorial undercurrent as described in previous literature

(Grenier et al., 2011). Samples were collected at the following depths: 10 m, 50 m, mixed layer as determined by CTD temperature profiles, 100 m, 150 m, 200 m, 250 m, 300 m, and 800 m. After collection, the nutrient samples were sent to the University of Washington Marine Chemistry lab for analysis of nitrate, phosphate and silicate concentrations. There, nutrients were analyzed following protocols from the [WOCE Hydrographic Program](#) using a Seal Analytical AA3. Minimum detection limits are: 0.18 μM for nitrate, 0.03 μM for phosphate, and 0.45 μM for silicate. Nutrient data was then interpolated from 5S -5N and 0-800m depth using a modified version of the code used to interpolate the density and temperature data (Cruz, 2024).

Density, Temperature, and CO_2

For the duration of the transect from 5S to 5N, fCO_2 , density and temperature data were continuously recorded using an underway CO_2 shipboard intake system from a depth of around 5 meters as described in Pierrot et al. (2009). To calculate mixed layer depth, the interpolated temperature data was used with the R function [Mixed Layer Depth](#) (Kaiser, 2020).

Fluorescence and Beam Transmission

Fluorescence and beam transmission (%) values for every sample bottle were obtained from the CTD for each cast. These variables, along with mixed layer depth, were compared to pCO_2 , nitrate, silicate and phosphate values using Pearson correlation analysis to determine possible correlations (Virtanen et al., 2020).

Historical Data

Historical data for surface pCO_2 was sourced from the [Surface Ocean \$\text{CO}_2\$ Atlas](#) as used in Yasunaka et al. (2019). pCO_2 data was calculated by converting the measured fugacity of CO_2

using the [f2pCO2](#) R script by Gattuso et al. (2021). The SOCAT pCO₂ data was filtered by year (year >= 1980), longitude (-175 <= longitude <= -160), and latitude (-5 <= latitude <= 5) to encapsulate the area around the transect.

Analysis

Statistical analyses were performed to quantify correlations. To understand the possible impacts of the ENSO cycle on pCO₂ concentration, pCO₂ data from the SOCAT database and pCO₂ data collected on the cruise were analyzed with ENSO sea surface temperature anomaly data obtained from the [NOAA Monthly Climate Time Series](#). A point biserial correlation analysis was performed on the data to determine correlation between ENSO state for January each year and average pCO₂ concentration each January using the Python package `scipy.stats` (Virtanen et al., 2020). To determine the overall trend of pCO₂ over time, a linear analysis was also performed on the pCO₂ data using the Python package `statsmodels.api` (Seabold & Perktold, 2010). To calculate correlation between atmospheric and surface pCO₂, atmospheric CO₂ was obtained from the [NOAA Global Monitoring Laboratory](#) and a Pearson correlation analysis was performed with the `scipy.stats` package. Over space, correlation was also calculated between nutrients and mixed layer depth, SST, fluorescence and beam transmission, and between pCO₂ and mixed layer depth, SST, fluorescence and beam transmission using the Pearson correlation analysis.

Results:

From 1983 to Jan. 2024, the average pCO₂ concentration in the western equatorial pacific (160–175 W, and 5S to 5N) exhibited an average increase of 2.02 ± 0.034 ppm/yr (Fig. 2). This

trend of increasing surface pCO₂ had a positive correlation ($R = 0.71$, $p\text{-value} < 0.001$) with globally averaged atmospheric pCO₂ increasing at 1.85 ± 0.009 ppm/yr ($p\text{-value} < 0.001$) (Fig. 2).

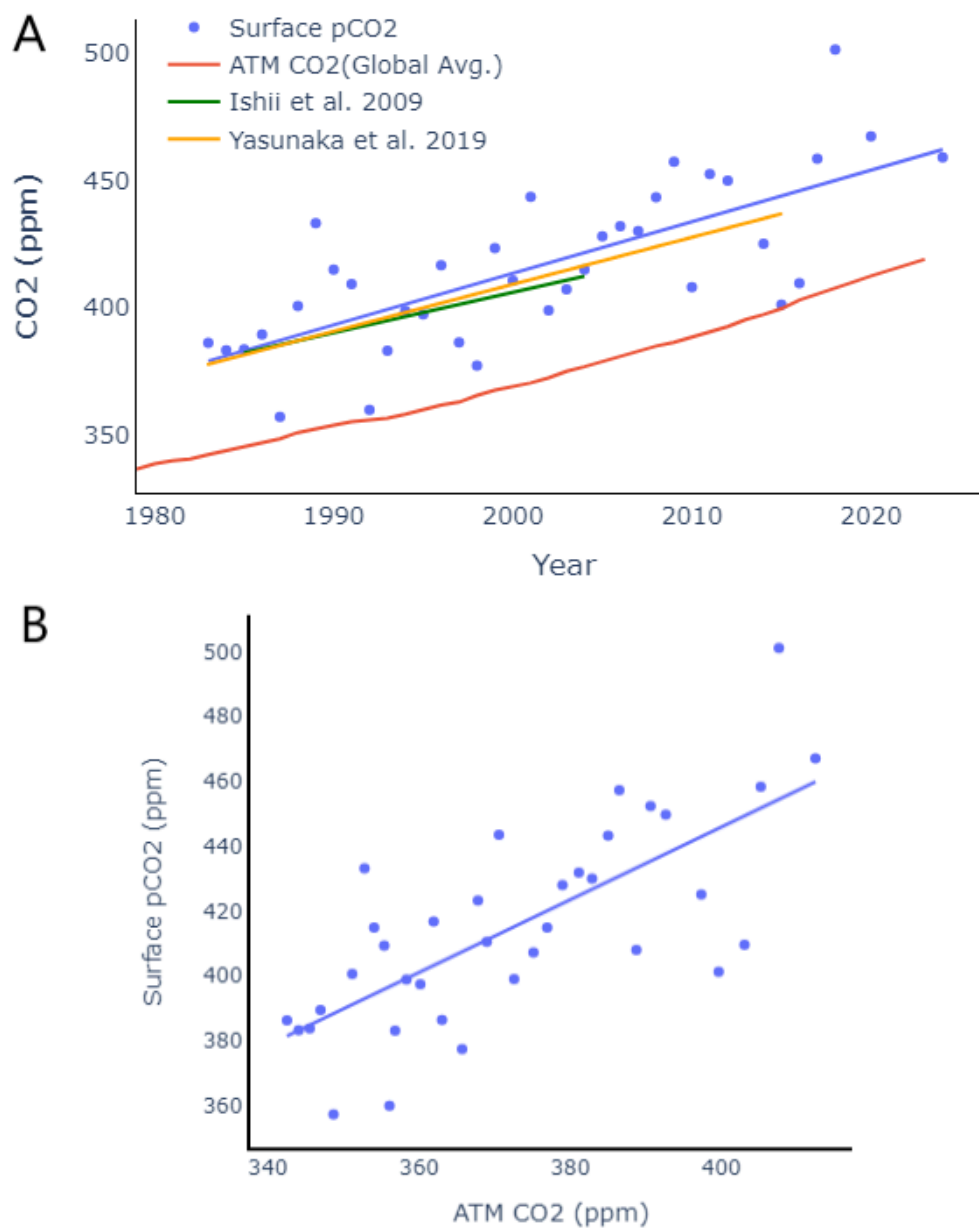


Figure 2. (A) Mean surface pCO₂ per year between 160W and 175 W and 5S to 5N and global average atmospheric CO₂ from 1983 to 2024. Trendlines of previously calculated pCO₂ rates using the same SoCAT data in green (Ishii et

al., 2009) and orange (Yasunaka et al., 2019). Atmospheric CO₂ values obtained from [NOAA Global Monitoring Laboratory](#). (B) Linear correlation between atmospheric CO₂ and surface pCO₂ concentration.

The calculated pCO₂ surface trend from 1983 - 2024 was compared to previous trends calculated from 1985-2004 (Ishii et al., 2009) and 1981-2015 (Yasunaka et al., 2019) (Fig. 2). While there was an increase in the calculated trend rates between the studies from 2009 to 2024, the trends were not significantly different based on the overlap of the calculated confidence intervals (95%) for all trendlines.

A point biserial correlation was run in order to determine if there was a correlation between the state of the ENSO cycle in January between 1983 and 2024 and the pCO₂ concentration in the equatorial pacific (140W-150E and 5S-5N). A slight negative correlation ($R = -0.36$, $p\text{-value} < 0.001$) was observed, indicating higher levels of pCO₂ during La Niña Januarys on average.

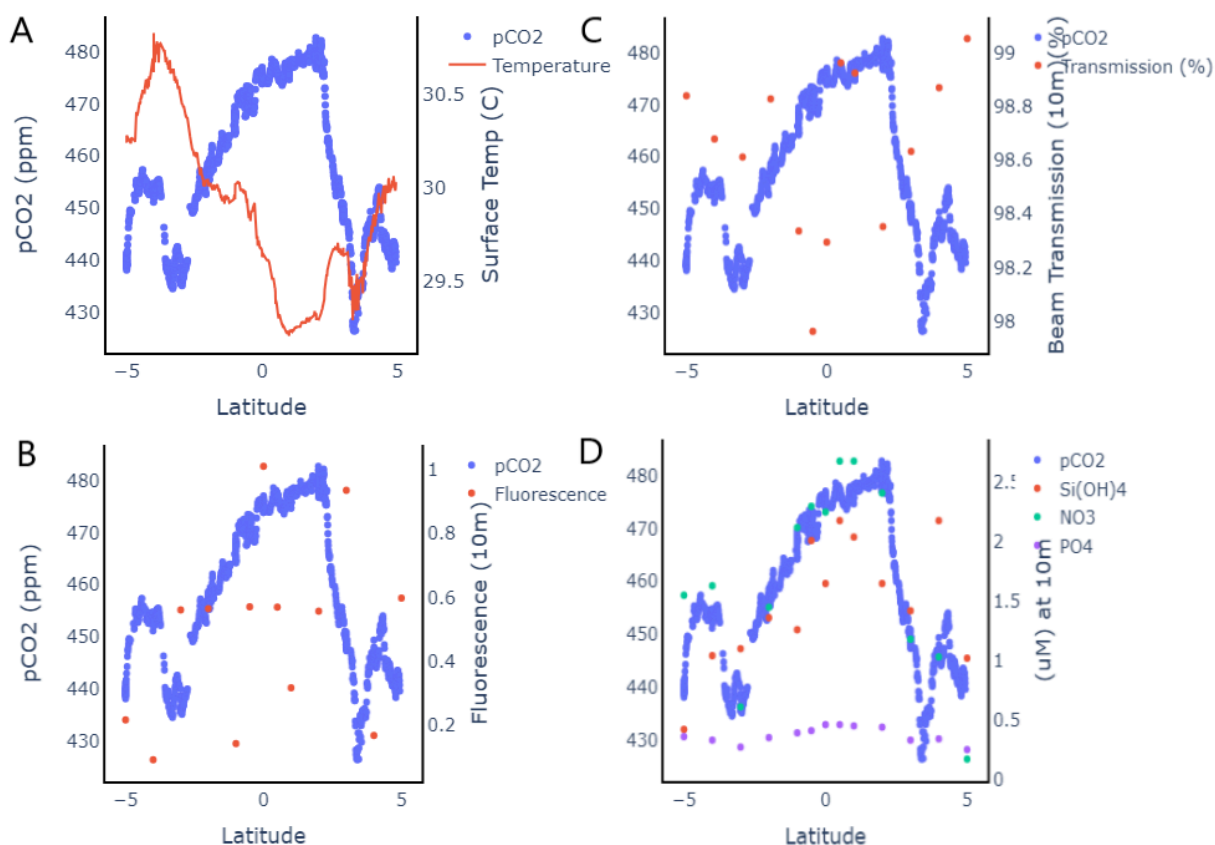


Figure 3. Surface pCO₂ concentration (ppm) plotted with (A) temperature (C°), (B) fluorescence at 10m, (C) beam transmission (%) at 10m, and (D) nutrient concentration at 10m (μ M), from 5S to 5N along 167W in early January, 2024.

When analyzed spatially, pCO₂ data obtained from the TN427 cruise along 167W shows a peak in pCO₂ from 0-2N at ~470-480 ppm (Fig. 3). pCO₂ levels consistently decrease to the north and south from the equator until around 3S (~435 ppm) and 3N (~425 ppm) whereupon concentrations begin to increase from 3-4 N and S (~455 ppm). After these secondary peaks, pCO₂ values decrease to the north and south along the transect line until 5N and 5S (Fig. 3). This creates a roughly symmetrical pattern of pCO₂ values along the transect.

When graphed with sea surface temperature over the transect, pCO₂ and temperature showed inverse trends near the equator and to the south of the equator, but both exhibit a minimum around 3N (Fig. 3). When analyzed with a Pearson correlation test, pCO₂ and

temperature had a negative correlation with an $R = -0.58$ and $p\text{-value} < 0.001$. $p\text{CO}_2$ and fluorescence had no correlation ($p\text{-value} > 0.05$) and $p\text{CO}_2$ and beam transmission also had no significant correlation ($p\text{-value} > 0.05$). Surface $p\text{CO}_2$ and nitrate concentrations at 10m had a significant positive correlation ($R = 0.92$, $p\text{-value} < 0.001$), and $p\text{CO}_2$ and phosphate also had a significant positive correlation ($R = 0.92$, $p\text{-value} < 0.001$). Surface $p\text{CO}_2$ and silicate at 10m had a weak but significant positive correlation ($R = 0.64$, $p\text{-value} = 0.02$). When analyzed with mixed layer depth, it was found that $p\text{CO}_2$ had a weak but significant negative correlation ($R = -0.32$, $p\text{-value} < 0.001$).

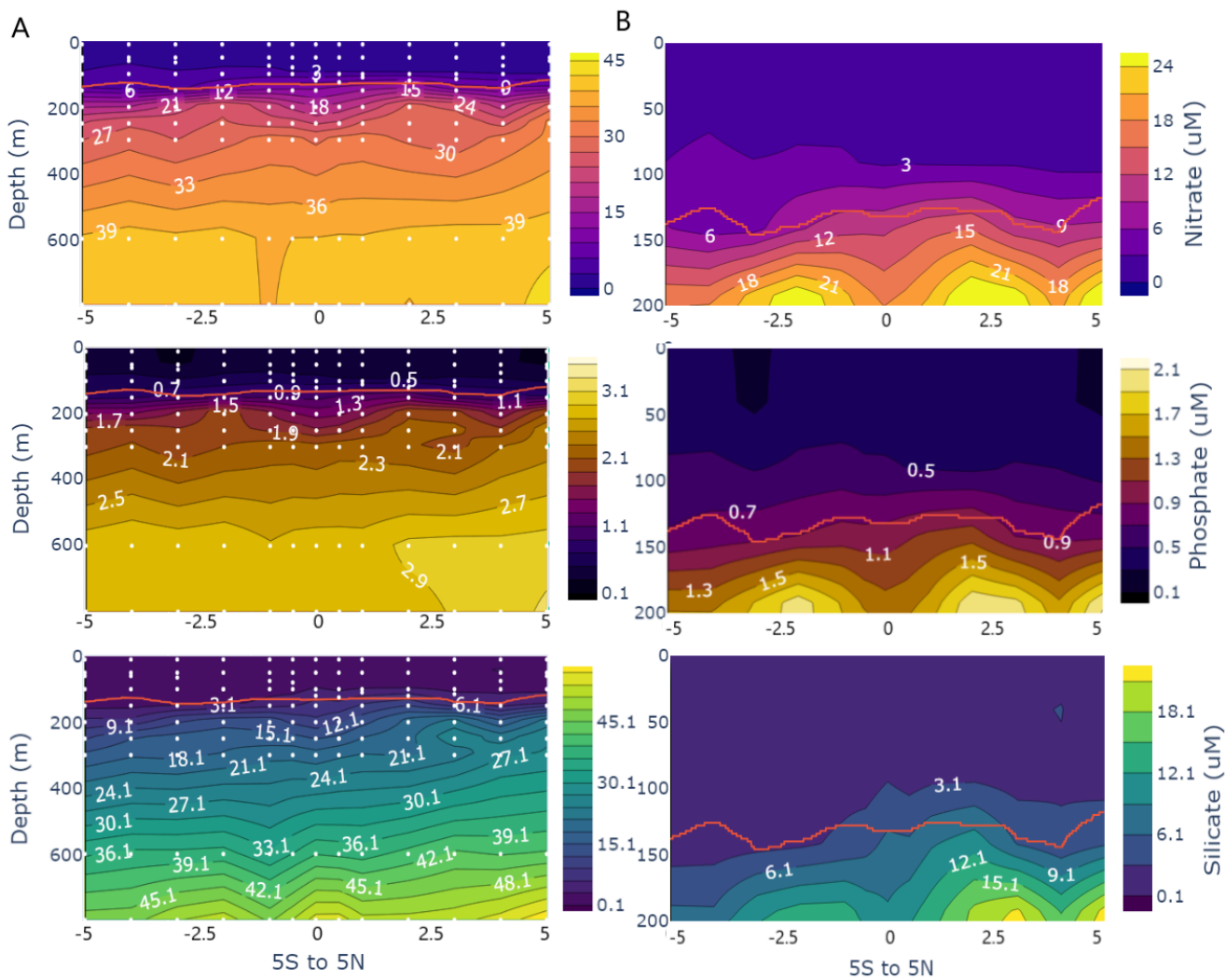


Figure 4. Nutrient depth profiles of nitrate, phosphate, and silicate in μM , from 5S to 5N along 167W from (A) 0-800 m and from (B) 0-200 m. Calculated mixed layer depth is notated as a red line. Nutrient sample locations are marked with points.

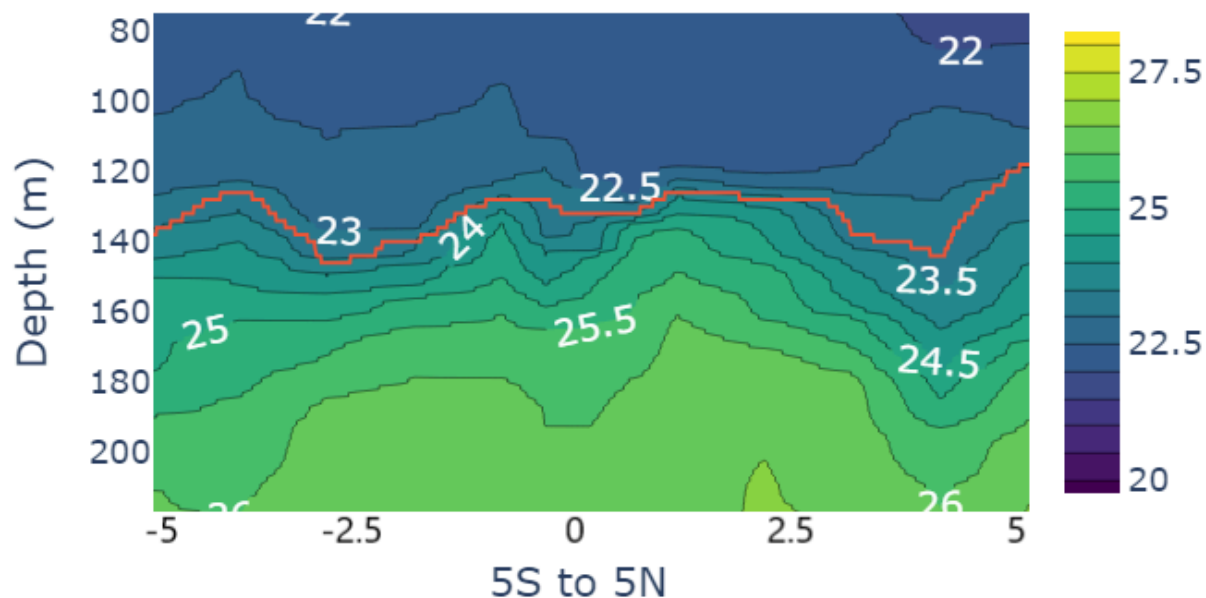


Figure 5. Density depth contour (kg/m^3) zoomed to highlight mixed layer depth, 5S to 5N along 167W .

Nutrient concentrations along the transect were low at the surface and high at depth, with a steep cline around 200m. In general, the low nutrient surface layer tended to be deepest around the equator and shallowest to the north and south of this zone, before deepening slightly closer to 3-4S and 3-4N (Fig. 4). The density mixed layer showed a similar pattern, though it remained shallow across the equator and expressed an increase in depth south of the equator closer to 2.5S (Fig 5.).

When analyzed against mixed layer depth using a Pearson correlation test, nitrate ($R = -0.43$, $p\text{-value} < 0.001$) and phosphate ($R = -0.40$, $p\text{-value} < 0.001$) concentrations in the mixed layer had low but significant negative correlations with mixed layer depth. However, silicate did not have a significant correlation with mixed layer depth ($p\text{-value} > 0.05$). When analyzed along the transect, nitrate ($R = -0.55$, $p\text{-value} < 0.001$), phosphate ($R = -0.70$, $p\text{-value} < 0.001$), and silicate ($R = -0.81$, $p\text{-value} < 0.001$) at 10m depth showed a negative correlation with interpolated SST values.

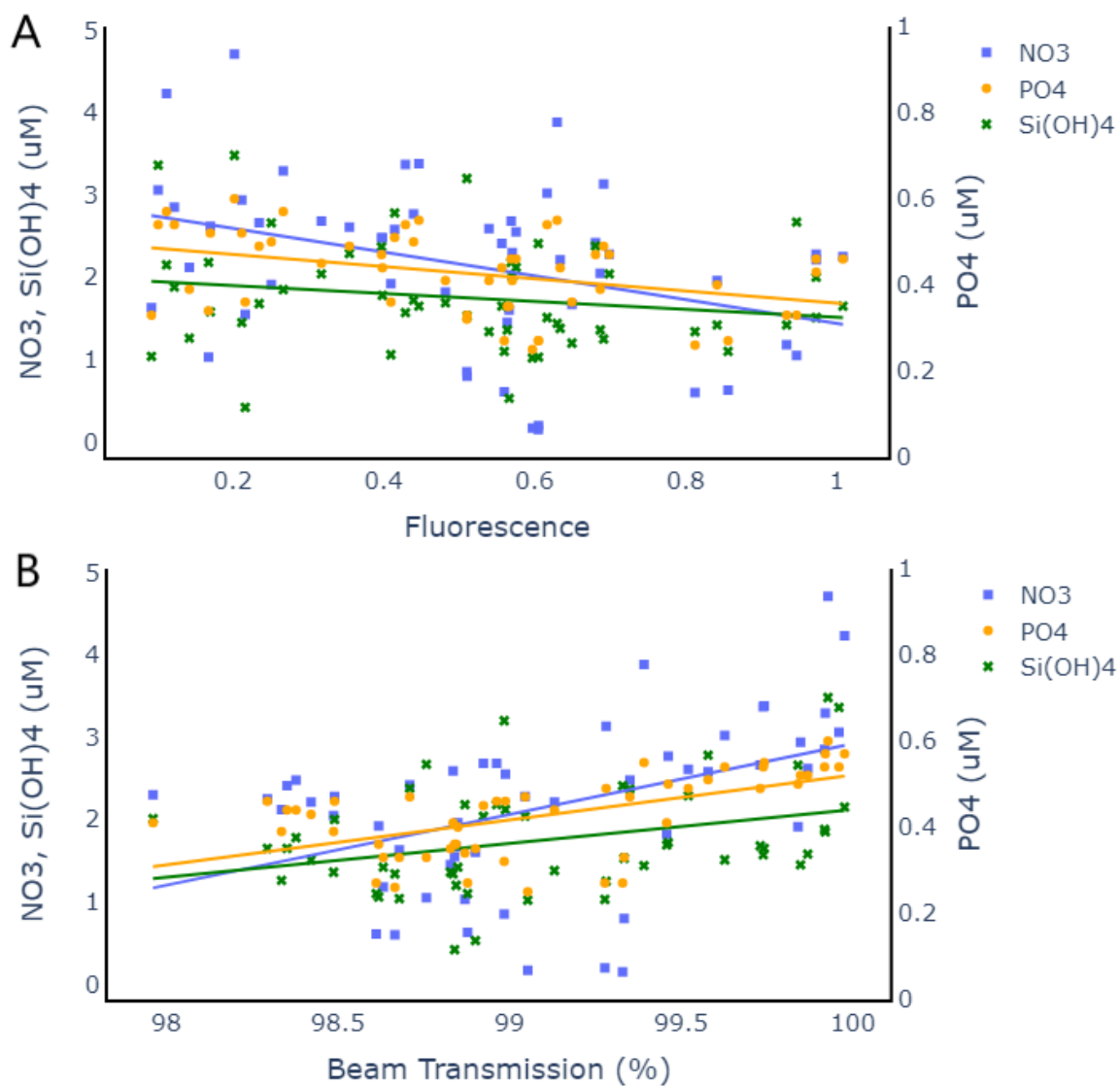


Figure 6. Fluorescence (A) and beam transmission (%) (B) versus concentration of nitrate, phosphate, silicate (μM), above 150m, 5S to 5N along 167W in early January, 2024.

When analyzed along the transect at depths above 150 m, there was a significant negative correlation between nitrate ($R = -0.36$, $p\text{-value} < 0.01$) and phosphate ($R = -0.38$, $p\text{-value} < 0.01$) concentration and fluorescence (Fig. 6). When a Pearson correlation was run across the entire water column there was a negative correlation between all nutrient concentrations, including silicate, and fluorescence ($p\text{-value} < 0.05$). Beam transmission was also compared to nutrient concentrations. Above 150m, it was found that nitrate ($R = 0.45$, $p\text{-value} < 0.001$), phosphate (R

= 0.59, p-value < 0.001), and silicate ($R = 0.34$, p-value < 0.05) had weak but significant positive correlations with beam transmission (Fig. 6). This correlation was stronger ($R > 0.6$), and more significant (p-value < 0.00001) when computed from 0-800m along the transect.

Discussion

The increase in western equatorial $p\text{CO}_2$ determined by this study (2.02 ± 0.034 ppm/yr) is slightly above the long-term average increase in $p\text{CO}_2$ across the equatorial region calculated by Yasunaka et al. (2019) from 1981 to 2015 of 1.84 ± 0.07 ppm/yr (Fig. 3). In the western equatorial Pacific specifically, it was previously calculated that the $p\text{CO}_2$ trend was between 1.5-2 ppm/yr, and most locations with $p\text{CO}_2$ trends of greater than 2 ppm/yr were found in the eastern equatorial region (Yasunaka et al., 2019). In an even earlier study, from 1985 to 2004 the calculated $p\text{CO}_2$ trend in the western equatorial Pacific was 1.5 ± 0.2 ppm/year (Ishii et al., 2009). The data from this study agrees with that of Yasunaka et al. (2019) and Ishii et al. (2009), indicating that there is an increase in surface $p\text{CO}_2$ values with time. Furthermore, the atmospheric trend calculated in this study was 1.85 ± 0.009 ppm/yr, slightly greater than the atmospheric average trend reported in Yasunaka et al. (2019) of 1.66 ± 0.01 ppm/yr. This trend in atmospheric CO_2 had a positive correlation with surface $p\text{CO}_2$ values ($R = 0.71$, p-value < 0.001), agreeing with the idea that surface $p\text{CO}_2$ concentration increase is influenced by atmospheric CO_2 concentrations (Sutton et al., 2014). Therefore, it is possible that an increase in CO_2 in the atmosphere is causing an increase in surface $p\text{CO}_2$ concentration in the western equatorial Pacific over time. This large correlation between surface $p\text{CO}_2$ and atmospheric CO_2 values disagrees with the proposed idea that the long term $p\text{CO}_2$ trends in the Pacific are mainly the product of the PDO forcing and are not influenced by atmospheric trends (Yasunaka et al.,

2019). However, in this study PDO forcing was not included in analysis as a possible driver of surface pCO₂ variability, and therefore cannot be ruled out.

The negative correlation ($R = -0.36$, $p\text{-value} < 0.001$) between ENSO state and pCO₂ concentration agrees with previous studies who also found increased pCO₂ and nutrients during La Niña years (Yasunaka et al., 2019; Wong et al., 1993). For instance, it was found that in La Niña years, pCO₂ became supersaturated leading to increased ocean-atmosphere CO₂ exchange ($> 70 \mu\text{atm}$), while during El Niño years pCO₂ decreased, reducing ocean-atmosphere exchange ($< 40 \mu\text{atm}$) (Ishii et al., 2009). This occurs because during La Niña years, strengthening of trade winds causes increased upwelling, bringing more pCO₂ and nutrient rich waters to the surface and therefore increasing the extent of the cold tongue to the west along the equator (Yasunaka et al., 2019; Wong et al., 1993; Feely et al., 1999; Ishii et al., 2009). This can cause the net sea-atmosphere carbon flux to increase, as more CO₂ is released into the atmosphere due to high sea surface concentrations (Pittman et al., 2022; Ishii et al., 2009). Meanwhile, CO₂ and nutrients concentrations decrease during El Niño years due to slowing of upwelling caused by decreased trade wind velocity (Yasunaka et al., 2019; Wong et al., 1993; Feely et al., 1999; Ishii et al., 2009).

Spatially, pCO₂ patterns were as expected from 5S to 5N based on the studies of Yasunaka et al. (2019) and Feely et al. (1999). In general, pCO₂ increased at the equator, and decreased to the north and south as reported in previous studies (Yasunaka et al., 2019; Feely et al., 1999) (Fig. 3). The peak in pCO₂ and corresponding low in SST at 0-2N (Fig. 3) is expected and corresponds with the previous data that indicates pCO₂ concentrations at the equator are primarily influenced by upwelling, and therefore have an inverse relationship with temperature (Yasunaka et al., 2019). This is further corroborated by the significant negative correlation found

between SST and surface $p\text{CO}_2$ ($R = -0.58$, $p\text{-value} < 0.001$). In addition, a correlation analysis between surface $p\text{CO}_2$ and mixed layer depth indicated a slight negative correlation ($R = -0.32$, $p\text{-value} < 0.001$), which is likely due to the shoaling of the mixed layer at the equator caused by upwelling. The variations in $p\text{CO}_2$ and SST observed from 3-5S and 3-5N (Fig. 3) may be caused by mixing which introduces deep, colder, $p\text{CO}_2$ rich water into the surface layer. This may be caused by turbulence due to the north and south subsurface countercurrents, which exist at around 3N and 3S respectively (Grenier et al., 2011). The mixed layer was deeper around 2.5S and 3-4N, which may be indicative of this mixing caused by the countercurrents (Fig. 5).

In order to determine correlations between $p\text{CO}_2$ and biological indicators, $p\text{CO}_2$ was compared with total microorganism biomass and photosynthetic microorganism biomass (using beam transmission and fluorescence as proxies) (Fig. 3). There was no significant correlation between either total biomass, or photosynthetic biomass, and $p\text{CO}_2$ ($p\text{-value} > 0.05$). This agrees with previous studies which have found that there is little if any direct correlation between biomass and CO_2 concentration (Tortell et al., 2002). This is because large amounts of $p\text{CO}_2$ rich upwelled water prevent depletion of CO_2 at the equator (Yasunaka et al., 2019).

$p\text{CO}_2$ was also compared with nitrate, phosphate and silicate concentrations at 10m in order to determine correlation (Fig. 3). All three nutrients had significant positive correlations with $p\text{CO}_2$. It has been shown by multiple studies that both CO_2 and nutrients at the surface in the equatorial pacific are primarily influenced by upwelling of deep water along the equator (Yasunaka et al., 2019; Sutton et al., 2014). Therefore, the correlation between nutrients and CO_2 that indicates they are both influenced by upwelling agrees with the established literature. While nitrate ($R = 0.92$) and phosphate ($R = 0.92$) had strong positive correlations ($p\text{-value} < 0.001$), the correlation between silicate and $p\text{CO}_2$ was slightly weaker ($R = 0.64$, $p\text{-value} = 0.02$). This

may be because silicate is depleted relative to $p\text{CO}_2$, nitrate and phosphate near the surface. Silicate can be a limiting nutrient in the equator when diatoms make up the majority of the phytoplankton community (Strutton & Chavez, 2000). This is because diatoms use silicate to build their internal structures (frustules) and therefore require more silicate than most other phytoplankton (Tilman et al., 1982). Diatoms, along with picoplankton, are one of the two assumed main groups of phytoplankton in the equatorial Pacific (Strutton et al., 2008). Depletion due to use by diatoms could explain why silicate is not correlated to the same extent as other nutrients and $p\text{CO}_2$ in the western equatorial Pacific.

Macronutrient concentrations were highest in deep water, and lowest at the surface (Fig. 4), as expected due to use by photosynthetic organisms in the photic zone and regeneration at depth (Tilman et al., 1982). The nutrient cline tended to extend across a wider range of depths near the equator, likely due to upwelling. To the north and south the low nutrient surface layer became shallower. There was a small but significant negative correlation between mixed layer depth, nitrate and phosphate concentration (p-value < 0.001) similar to $p\text{CO}_2$. This is likely due to the shoaling of the mixed layer at the equator (Fig. 5) which corresponds with upwelling of nutrient rich water (Yasunaka et al., 2019). This is further supported by the negative correlations between the nutrient concentration and SST (p-value < 0.001). As lower SST values near the equator are caused by upwelling. However, there was no correlation between mixed layer depth and silicate (p-value > 0.05). Once again, this may be due to relatively high silicate depletion along the transect in surface waters from phytoplankton uptake (Strutton & Chavez, 2000). There was a small but noticeable increase in concentration (most pronounced for phosphate) at 200m around 3-4 N and S (Fig. 4). This, similar to the peaks seen in the $p\text{CO}_2$ data (Fig. 3) and the changes in the density mixed layer at 2.5S and 3-4N (Fig. 5), may be caused by increased mixing

from the subsurface counter currents present to the north and south of the equator (Grenier et al., 2011).

In order to determine possible correlations between nutrient concentrations and biomass, correlation analyses were performed between nutrients, beam transmission and fluorescence (Fig. 6). When performed over the top 150m, there was a negative correlation between nitrate, phosphate and photosynthetic microorganism biomass (p-value < 0.01) (Fig. 6). This correlation was also observed in silicate (p-value < 0.05) when analyzed from 0-800 meters along the transect. This is likely because nutrients are highest in deep water where they are regenerated by respiration, and lowest near the surface where they are used by photosynthetic organisms, whereas fluorescence is highest near surface due to the presence of photosynthetic organisms (Tilman et al., 1982). When compared with total microorganism biomass, all nutrients, nitrate ($R = 0.45$, p-value < 0.001), phosphate ($R = 0.59$, p-value < 0.001), and silicate ($R = 0.34$, p-value < 0.05), had weak but significant positive correlations above 150m (Fig. 6). These correlations become stronger and more significant when observed from 0-800 m (p-value < 0.00001) (Fig. 6). This is likely because beam transmission and nutrients increased with depth due to the presence of organisms near the surface which lower beam transmission and can take up nutrients (Tilman et al., 1982). It is possible that silicate has a weaker correlation to total microorganism biomass than nitrate and phosphate above 150m because it is a limiting nutrient and is therefore depleted relative to nitrate and phosphate throughout the surface water (Strutton & Chavez, 2000).

Conclusion:

This study found a positive trend of $p\text{CO}_2$ in the surface water of the western equatorial pacific (2.02 ± 0.034 ppm/yr), and a significant correlation between the trend of $p\text{CO}_2$

concentration in surface water and the global average atmospheric concentration ($R = 0.71$, $p\text{-value} < 0.001$). Therefore, while ocean surface $p\text{CO}_2$ can be affected by oscillations such as ENSO and the PDO at differing timescales, it is likely that increased atmospheric CO_2 has a significant impact on long term $p\text{CO}_2$ trends in the western equatorial Pacific. Spatially, in the western Pacific $p\text{CO}_2$ is most impacted by upwelling at the equator, and likely mixing from north and south subsurface counter currents at 3-4N and S. Similarly, macronutrients nitrate, phosphate, and silicate, seem to be predominantly influenced by upwelling at the equator. This indicates that physical factors, rather than biological processes, are likely the dominant drivers of $p\text{CO}_2$ and nutrient variation in the western equatorial Pacific. Future observations of $p\text{CO}_2$ and nutrients in the region may confirm temporal trends and elucidate how the region may be impacted by increasing atmospheric $p\text{CO}_2$ and changing physical parameters due to climate change.

Acknowledgements:

Special thanks to the captain, crew, and marine techs aboard the RV Thomas G. Thompson, the professors of OCEAN 443-445 series, and my peers. Thanks to my classmate Cody Cruz, who wrote an interpolation code which was used as a basis for the code used to interpolate the nutrient data. Thanks also to the NOAA-PMEL lab, directed by Simone Alin, which provided access to the cruise $p\text{CO}_2$ data.

References

- Archer, D., Takahashi, T., Sutherland, S. C., Goddard, J., Chipman, D., Rodgers, K. B., & Ogura, H. (1996). Daily, seasonal and interannual variability of sea-surface carbon and nutrient concentration in the equatorial Pacific Ocean. *Deep Sea Research Part II: Topical Studies in Oceanography*, 43(4–6), 779–808. [https://doi.org/10.1016/0967-0645\(96\)00017-3](https://doi.org/10.1016/0967-0645(96)00017-3)
- Barber, R., Murray, J., & McCarthy, J. (1994). Biogeochemical Interactions in the Equatorial Pacific. *Ambio*, 23(1), 62–66. <https://www.jstor.org/stable/4314162>
- Bjerknes, J. (1969). Atmospheric teleconnections from the Equatorial Pacific. *Monthly Weather Review*, 97(3), 163–172. [https://doi.org/10.1175/1520-0493\(1969\)097](https://doi.org/10.1175/1520-0493(1969)097)
- Cruz, C. (2024). GitHub - GHOpenonic/equatorial-pacific-turbulent-mixing. Retrieved from <https://github.com/GHOpenonic/equatorial-pacific-turbulent-mixing>
- Feely, R. A., Wanninkhof, R., Takahashi, T., & Tans, P. P. (1999). Influence of El Niño on the equatorial Pacific contribution to atmospheric CO₂ accumulation. *Nature*, 398(6728), 597–601. <https://doi.org/10.1038/19273>
- Gattuso J. P., Epitalon J. M., Lavigne H. & Orr J., (2021) seacarb: seawater carbonate chemistry. R package version 3.3.0. <http://CRAN.R-project.org/package=seacarb>
- Gierach, M. M., Lee, T., Turk, D., & McPhaden, M. J. (2012). Biological response to the 1997-98 and 2009-10 El Niño events in the equatorial Pacific Ocean. *Geophysical Research Letters*, 39(10), n/a. <https://doi.org/10.1029/2012gl051103>
- Grenier, M., Cravatte, S., Blanke, B., Menkès, C. E., Koch-Larrouy, A., Durand, F., et al. (2011). From the western boundary currents to the Pacific Equatorial Undercurrent: Modeled pathways and water mass evolutions. *Journal of Geophysical Research*, 116(C12). <https://doi.org/10.1029/2011jc007477>

- Ishii, M., Inoue, H., Midorikawa, T., Saito, S., Tokieda, T., Sasano, D., et al. (2009). Spatial variability and decadal trend of the oceanic CO₂ in the western equatorial Pacific warm/fresh water. *Deep Sea Research Part II: Topical Studies in Oceanography*, 56(8–10), 591–606. <https://doi.org/10.1016/j.dsr2.2009.01.002>
- Jin, F. (1997). A theory of interdecadal climate variability of the North Pacific Ocean–Atmosphere System. *Journal of Climate*, 10(8), 1821–1835. [https://doi.org/10.1175/1520-0442\(1997\)010](https://doi.org/10.1175/1520-0442(1997)010)
- Kaiser, D. (2020). GitHub - Davidatlarge/mixed_layer_depth: calculate the depth of the surface mixed layer of a water column. Retrieved from https://github.com/Davidatlarge/mixed_layer_depth
- Kang, S. M., Shin, Y., Kim, H., Xie, S., & Hu, S. (2023). Disentangling the mechanisms of equatorial Pacific climate change. *Science Advances*, 9(19). <https://doi.org/10.1126/sciadv.adf5059>
- Kessler, W. S., & McPhaden, M. J. (1995). The 1991–1993 El Niño in the central Pacific. *Deep Sea Research Part II: Topical Studies in Oceanography*, 42(2–3), 295–333. [https://doi.org/10.1016/0967-0645\(95\)00041-n](https://doi.org/10.1016/0967-0645(95)00041-n)
- Meyer, J., & Riebesell, U. (2015). Reviews and Syntheses: Responses of coccolithophores to ocean acidification: a meta-analysis. *Biogeosciences*, 12(6), 1671–1682. <https://doi.org/10.5194/bg-12-1671-2015>
- Murray, J., Leinen, M., Feely, R. A., Toggweiler, R., & Wanninkhof, R. (1992). EQPAC: A process study in the Central Equatorial Pacific. *Oceanography*, 5(3), 134–142. <https://doi.org/10.5670/oceanog.1992.01>

- Newman, M., Alexander, M. A., Ault, T. R., Cobb, K. M., Deser, C., Di Lorenzo, E., et al. (2016). The Pacific Decadal Oscillation, revisited. *Journal of Climate*, 29(12), 4399–4427. <https://doi.org/10.1175/jcli-d-15-0508.1>
- Paytan, A., & Hönlisch, B. (2016). Ocean acidification - A paleo perspective. *Limnology and Oceanography E-Lectures*, 6(2), 1–49. <https://doi.org/10.1002/loe2.10003>
- Pierrot, D., Neill, C., Sullivan, K., Castle, R., Wanninkhof, R., Lüger, H., Johannessen, T., Olsen, A., Feely, R. A., & Cosca, C. E. (2009). Recommendations for autonomous underway pCO₂ measuring systems and data-reduction routines. *Deep Sea Research Part II: Topical Studies in Oceanography*, 56(8–10), 512–522.
- Pittman, N. A., Strutton, P. G., Johnson, R. W., Matear, R. J., & Sutton, A. J. (2022). Relationships between air-sea CO₂ flux and new production in the equatorial Pacific. *Global Biogeochemical Cycles*, 36(4). <https://doi.org/10.1029/2021gb007121>
- Seabold, S., & Perktold, J. (2010). Statsmodels: Econometric and Statistical Modeling with Python. *Proceedings of the Python in Science Conferences*. <https://doi.org/10.25080/majora-92bf1922-011>
- Steele, J. H., & Frost, B. W. (1977). The structure of plankton communities. *Philosophical Transactions of the Royal Society of London*, 280(976), 485–534. <https://doi.org/10.1098/rstb.1977.0119>
- Stramma, L., Fischer, T., Grundle, D. S., Krahnemann, G., Bange, H. W., & Marandino, C. (2016). Observed El Niño conditions in the eastern tropical Pacific in October 2015. *Ocean Science*, 12(4), 861–873. <https://doi.org/10.5194/os-12-861-2016>

- Strutton, P. G., & Chávez, F. P. (2000). Primary productivity in the equatorial Pacific during the 1997–1998 El Niño. *Journal of Geophysical Research*, *105*(C11), 26089–26101.
<https://doi.org/10.1029/1999jc000056>
- Strutton, P. G., Evans, W., & Chávez, F. P. (2008). Equatorial Pacific chemical and biological variability, 1997–2003. *Global Biogeochemical Cycles*, *22*(2).
<https://doi.org/10.1029/2007gb003045>
- Sutton, A. J., Feely, R. A., Sabine, C. L., McPhaden, M. J., Takahashi, T., Chávez, F. P., et al. (2014). Natural variability and anthropogenic change in equatorial Pacific surface ocean $p\text{CO}_2$ and pH. *Global Biogeochemical Cycles*, *28*(2), 131–145.
<https://doi.org/10.1002/2013gb004679>
- Talling, J. F. (1976). The Depletion of Carbon Dioxide from Lake Water by Phytoplankton. *Journal of Ecology*, *64*(1), 79. <https://doi.org/10.2307/2258685>
- Tilman, D., Kilham, S. S., & Kilham, P. (1982). Phytoplankton Community ecology: The role of limiting nutrients. *Annual Review of Ecology and Systematics*, *13*(1), 349–372.
<https://doi.org/10.1146/annurev.es.13.110182.002025>
- Tortell, P. D., DiTullio, G. R., Sigman, D. M., & Morel, F. M. M. (2002). CO_2 effects on taxonomic composition and nutrient utilization in an Equatorial Pacific phytoplankton assemblage. *Marine Ecology Progress Series*, *236*, 37–43.
<https://doi.org/10.3354/meps236037>
- Virtanen, P., Gommers, R., Oliphant, T. E., Haberland, M., Reddy, T., Cournapeau, D., et al. (2020). SciPy 1.0: fundamental algorithms for scientific computing in Python. *Nature Methods*, *17*(3), 261–272. <https://doi.org/10.1038/s41592-019-0686-2>

Wong, C. S., Chan, Y., Page, J. S., Smith, G. E., & Bellegay, R. D. (1993). Changes in equatorial CO₂ flux and new production estimated from CO₂ and nutrient levels in Pacific surface waters during the 1986/87 El Niño. *Tellus B*, 45(1), 64.

<https://doi.org/10.3402/tellusb.v45i1.15580>

Yasunaka, S., Kouketsu, S., Strutton, P. G., Sutton, A. J., Murata, A., Nakaoka, S. I., & Nojiri, Y. (2019). Spatio-temporal variability of surface water pCO₂ and nutrients in the tropical Pacific from 1981 to 2015. *Deep Sea Research Part II: Topical Studies in Oceanography*, 169–170, 104680. <https://doi.org/10.1016/j.dsr2.2019.104680>